

## Establishment of patient-derived xenografts of retinoblastoma and choroidal melanoma on the avian chorioallantoic membrane

Nimita Kant, Perumal Jayaraj<sup>1</sup>, Seema Sen<sup>2</sup>, Harshita Rupani<sup>1</sup>, Pranavi Kumar<sup>1</sup>, Shefali Dahiya<sup>1</sup>, Palak Chugh<sup>1</sup>, Muskaan Gupta<sup>1</sup>, Manisha Sengar<sup>3</sup>

**Purpose:** To develop a viable *in vivo* chorioallantoic membrane (CAM) model to study the growth and invasion of patient-derived retinoblastoma (RB) and choroidal melanoma (CM) xenografts (PDXs). The study utilizes primary tumor samples instead of cancer cell lines, which provides a more authentic representation of tumors due to conserved morphology and heterogeneity. **Methods:** Fertilized chicken eggs were procured, windowed, and their CAM layers were dropped. On embryonic development day (EDD) 10, freshly cut patient-derived CM and RB tumors were implanted on the CAM layer and the setup was incubated for 7 days. The tumor-embedded CAM layer was harvested on EDD 17, and the extracted tumor samples were subjected to hematoxylin and eosin staining and immunohistochemical analysis to evaluate the extent of tumor invasion. **Results:** Significant changes in the vascularity around the RB and CM PDXs were observed, indicating an angiogenic environment. The cross-sectional histological view of the tumor implant site revealed the invasion of both the tumors into the CAM mesoderm. Invasion of CM into CAM mesoderm was visualized in the form of pigmented nodules, and that of RB was indicated by synaptophysin and Ki-67 positivity in Immunohistochemistry (IHC). **Conclusion:** The CAM xenograft model was successfully able to support the growth of CM and RB PDXs and their invasion in CAM, thus presenting as a feasible alternative to mammalian models for studying tumorigenicity and invasiveness of ocular tumors. Moreover, this model can further be utilized to develop personalized medicine by inoculating patient-specific tumors for preclinical drug screening.

**Key words:** CAM, chicken, chorioallantoic membrane, choroidal melanoma, eye cancer, ocular cancer, patient-derived xenograft, retinoblastoma, uveal melanoma

Uveal melanoma (UM), arising from the melanocytes of the uveal tract, is the most common cause of primary malignant intraocular neoplasm in the western world.<sup>[1]</sup> It originates from iris (4%), ciliary body (6%), or choroid (85%–90%), the latter being the most prevalent form.<sup>[2]</sup> UM is characteristically distinct from cutaneous melanoma which originates from the melanocytes confined within the basal layer of the epidermis.<sup>[3]</sup> Prognosis and metastasis of all UMs are majorly affected by mutations in *GNAQ* and *GNA11* genes.<sup>[4]</sup> Nearly 50% of the afflicted individuals succumb to metastasis within 10 years of diagnosis.<sup>[5]</sup>

Choroidal melanoma (CM) accounts for more than 70% cases of UM, rendering it the second most predominant form of malignant tumors. Despite the advancement in therapeutics, the median survival of patients with CM is less than a year.<sup>[6]</sup> Its common metastatic sites are the liver (90%), lungs (24%), and

bones (16%) owing to its heterogeneous spread.<sup>[1]</sup> Depending on the extent of tumor growth, its treatment could vary from brachytherapy, endoresection, exoresection to the complete removal of the eyeball.<sup>[6,7]</sup> High metastatic potential and low survival incidence of CM make it more pertinent to oncology research.

Among children, retinoblastoma (RB) is the most widespread intraocular tumor, arising in both heritable and nonheritable forms, accounting for approximately 8000 cases annually.<sup>[8,9]</sup> It is caused by a mutation in both RB1 alleles in a retinal cell; early lesions of RB are found in the inner nuclear layer of the retina.<sup>[10,11]</sup> Like UM, it is also metastatic in nature and if left untreated, it is highly likely to spread outside the eye and invade the central nervous system via the optic nerve. Through metastases in the bloodstream, it can also spread in regional lymph nodes, bones, lungs, and liver, making it very important to study its characteristics.<sup>[12,13]</sup>

Department of Zoology, Shivaji College, University of Delhi, New Delhi, <sup>1</sup>Department of Zoology, Sri Venkateswara College, University of Delhi, Delhi, <sup>2</sup>Department of Ocular Pathology, Dr. Rajendra Prasad Centre for Ophthalmic Science, All India Institute of Medical Science, New Delhi, <sup>3</sup>Department of Zoology, Deshbandhu College, University of Delhi, New Delhi, India

**Correspondence to:** Dr. Perumal Jayaraj, Department of Zoology, Sri Venkateswara College (University of Delhi), Benito Juarez Road, Dhaula Kuan, Delhi, India. E-mail: jay.aiims@gmail.com

Received: 23-Jun-2022

Revision: 22-Nov-2022

Accepted: 12-Dec-2022

Published: 03-Mar-2023

Access this article online

Website:

www.ijo.in

DOI:

10.4103/ijo.IJO\_1494\_22

Quick Response Code:



This is an open access journal, and articles are distributed under the terms of the Creative Commons Attribution-NonCommercial-ShareAlike 4.0 License, which allows others to remix, tweak, and build upon the work non-commercially, as long as appropriate credit is given and the new creations are licensed under the identical terms.

**For reprints contact:** WKHLRPMedknow\_reprints@wolterskluwer.com

**Cite this article as:** Kant N, Jayaraj P, Sen S, Rupani H, Kumar P, Dahiya S, et al. Establishment of patient-derived xenografts of retinoblastoma and choroidal melanoma on the avian chorioallantoic membrane. *Indian J Ophthalmol* 2023;71:977-82.

Extensive efforts have been devoted to developing an ideal model to study metastasis of UM and RB. This is primarily done using established UM and RB cancer cell lines on nude mice models and transendothelial, Transwell, and Matrigel invasion assays.<sup>[14–18]</sup> However, each of these models has its own disadvantages, like the Matrigel invasion assay is extensively attributed to variability and the nude mice model needs to be artificially immunocompromised and fails to lay out a natural environment for tumor development.<sup>[19,20]</sup> The chorioallantoic membrane (CAM) assay offers to be an admissible alternative to the above-mentioned models and can be employed to study tumor invasion in real time and it, together with extracellular matrix protein (ECM), imitates the true microenvironment of the basement membrane, allowing for tumor development.<sup>[21]</sup> Chick CAM is an extraembryonic structure identical to the placenta in mammals. It serves as the primary site for the gaseous exchange and also protects the chicken embryo during its development.<sup>[22]</sup> CAM is formed due to the fusion of mesodermal layers of chorion and allantois. Its rich vascular network and immune-naïve nature make it an exemplary substrate for tumor cultivation and angiogenesis study. Its high reproducibility, short incubation time, simple setup, and cost-effectiveness make it more ideal compared to conventional animal models.<sup>[23]</sup>

Recent studies have underlined the implication of utilizing xenograft in understanding metastasis. Most of this research involves the use of UM cell lines, namely OMM1 and 92.1, and RB cell lines, namely RB-Y79, WERI-RB1, and RB-355.<sup>[24,25]</sup> However, the xenograft model of CM and RB on CAM has been less utilized. Solid primary tissue has an edge over cell lines as it is a true representation of the actual tumor and conserves heterogeneity of tumor cell subpopulation.<sup>[26]</sup> Furthermore, results from xenograft of hepatocellular carcinoma, oral and laryngeal squamous cell carcinoma on CAM have established its success to study tumor invasion.<sup>[27–29]</sup>

This research aims to study the survival and tumor invasion of CM and RB xenograft on CAM and provides a basis for a potential future approach about their invasiveness and metastatic potential.

## Methods

### Egg procurement and preparation

An overview of the protocol has been presented in Fig. 1.

Fertilized eggs of *Gallus domesticus* were procured and cleaned using sterile water and paper towels. Following this, the eggs were maintained in an upright position under suitable conditions of 37.5°C temperature and 55%–60% relative humidity in order to maintain controlled conditions for embryogenesis throughout the study. The CAM assay was performed between the chick embryonic development day (EDD) 9 and 17. On EDD 9, the CAM tissue was identified. Further, the eggs were cleaned with distilled water, followed by which the air sac was punctured using a 19 G needle and a suction force was applied for the dropping of CAM. A window of 1.5 cm diameter was established on the upper surface of the eggs under aseptic conditions, and all the embryos were examined for any signs of local bleeding. Next, a sterile silicone o-ring (inner and outer diameter 8 and 10 mm, respectively) was placed onto the CAM in an area with visible vascularization.

### Tumor procurement and preparation

Fresh tumor tissues of CM and RB were obtained from two patients undergoing enucleation from the operation theater of Dr. R. P. Centre, All India Institute of Medical Sciences (AIIMS), New Delhi, India, after written and informed consent from donor patients and approval from the institutional ethics review board of AIIMS, New Delhi (IEC299/01.06-2018) were obtained and kept in isotonic saline solution at ambient temperatures of 18°C–20°C maintained by an insulated cool box. The tumors were then dissected with a sterile scalpel and a blade within a biosafety cabinet and were implanted in the chick CAM within a biosafety cabinet using sterile forceps. Patients receiving chemotherapy and brachytherapy were excluded from this study.

The tumor sample procured from the patient with CM (Stage IV) was divided into three tissue segments (replicates) of approximately 4–5 mm length, and the same step was followed for the tumor sample procured from the patient with RB (Group D). The replicates were excised with minimal disruption of the ocular architecture using a scalpel and a blade. The rest of the tumor tissue was formalin fixed and paraffin embedded for light microscopy and immunohistochemistry. The patient-derived xenografts (PDXs) were then subjected to CAM assay in separate setups. On EDD 10, each excised replicate of CM and RB was placed separately in the middle of a sterile silicone o-ring on the CAM of the egg after 45–60 min of enucleation. The egg windows were resealed with a sterile tape. The CAM using fertilized eggs of *G. gallus domesticus* minimizes the use of animal models and following the “3R” rule (replacement, refinement, and reduction), the CAM assay provides an excellent intermediary step before preclinical evaluation.

The animal experiment was carried out after approval was obtained from the institutional ethical and safety committee of Shivaji College, University of Delhi, New Delhi, India (Bioethics and Biosafety Committee Report, SCS2019).

### PDXs and CAM assay

The six inoculated eggs containing the PDX were placed back in the incubator, maintaining them in an undisturbed state for 7 days until EDD 17. On EDD 17, the chick was euthanized by inducing hypothermia. Following this, the CAM tissue bearing the PDX was extracted and washed with phosphate-buffered saline (PBS) to remove the remnants of yolk and extraembryonic membranes. The observations were then made under a stereoscopic microscope and photographs were taken. Shortly after this, the extracted tissue bearing the tumor sample was fixed in 3.7% paraformaldehyde for further processing.

### Histopathologic investigation

Following fixation and processing of the CAM tissue bearing the tumor, standard protocols were used for performing hematoxylin and eosin (H/E) staining on the sections. The sections were mounted, and imaging was performed using light microscopy. H/E-stained sections were then evaluated by an ophthalmic pathologist and two observers. The tumor invasion was shown to be represented by the occurrence of invasive cancer cells in the mesoderm of CAM on histologic sections' analysis.

### Immunohistochemistry

Paraffin-embedded and formalin-fixed tissue segments were mounted on poly-L-lysine microscope adhesion slides. Next, deparaffinization was performed by utilizing xylene,

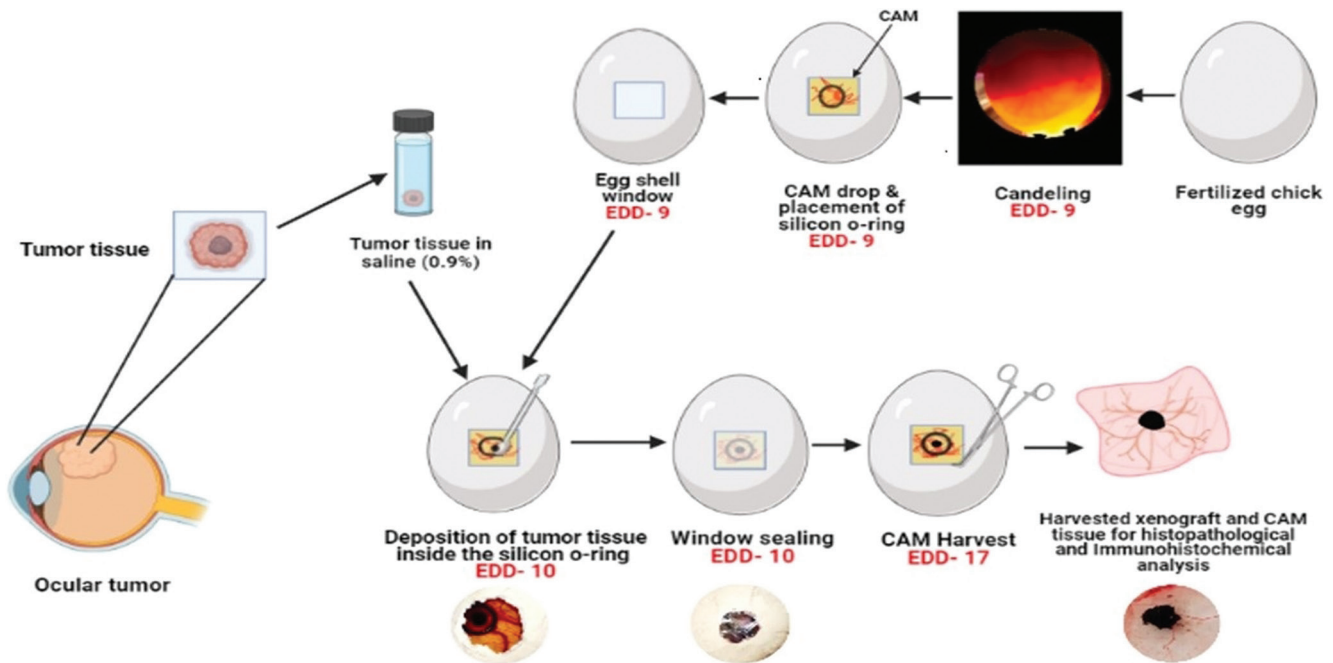


**Figure 1:** A schematic representation of the protocol followed to study CM and RB xenografts on CAM model. CAM = chorioallantoic membrane, CM = choroidal melanoma, RB = retinoblastoma

following which rehydration was achieved using a series of graded alcohols. After this, antigen retrieval was performed by incubating the tumor sections for approximately 20 min at a temperature of 90°C in citrate buffer of pH 6.0. The slides were then allowed to cool, after which they were washed with Tris-buffered saline of pH 7.5, and the endogenous peroxidase activity of the tumor sections was stopped by incubating them in H<sub>2</sub>O<sub>2</sub> (0.3% v/v) for 20 min. The RB xenograft tissue and associated CAM tissue sections were then incubated with monoclonal anti-synaptophysin antibody (MA5-14532, Thermo Fisher) and anti-Ki-67 antibody (MA5-14520, Thermo Fisher) at a dilution of 1:200. The immunoreactive signals were identified using the substrate DAB (3,3'-diaminobenzidine) (DAB) peroxidase. Hematoxylin was used as a counterstain for 30 s, following which the tissue sections were dehydrated and Dibutylphthalate Polystyrene Xylene (DPX) was utilized for mounting them. The results were demonstrated using light microscopy.

## Results

RB and CM PDXs were successfully grafted onto the CAM in all three replicates and were viable throughout the duration of the experiment, that is, until EDD 17, after which the CAM tissue bearing the tumor was excised. Gross visual assessment post-H/E staining demonstrated the development of dense vasculature around RB and CM PDXs postincubation, indicating an angiogenic microenvironment. The morphology of RB cells invading CAM resembled the native patient-derived tumor on gross visual microscopic observation, indicating successful invasion. In the case of melanoma cells, the spindle-shaped morphology of the surface cells of the CAM-invading tumor was the same as the original tumor xenograft.

Growth of blood vessels and high vascularization were observed over the side and underside of the tumor

[Figs. 2 and 3]. The cross-sectional histologic view of the control sample which lacked the tumor implant revealed a three-layered structure composed of ectoderm, mesoderm, and endoderm [Fig. 2]. H/E staining of CM tumor cell mass implanted on CAM further revealed that tumor cells adhered to CAM ectoderm and showed prominent invasion to the mesoderm [Fig. 2]. The invading cells in the mesoderm were visualized due to the pigmentation in melanoma cells and appeared as cleaving pigmented tumor nodules [Fig. 2]. H/E staining of RB cells was similar to CM cells, with the bulk of tumor cells adhering to CAM ectoderm and certain cells invading the CAM mesoderm [Fig. 3]. The only difference observed was in the degree of invasion, which was lesser compared to CM cells.

Immunohistochemical analysis was performed using synaptophysin and Ki-67 antibodies to confirm the identity of invading human RB cells. Invading cells in CAM mesoderm were positive for synaptophysin in the membrane and Ki-67 in the nucleus, thus confirming that the invading cells are patient derived and retain the hallmarks of RB cells [Fig. 3]. Overall, both RB and CM PDXs demonstrated a consistent adherence and cell invasion in all the samples.

## Discussion

Invasion and metastasis are frequent and often a life-threatening transformation for RB and CM patients. The chick chorioallantoic membrane fosters tumor growth and administers an assisting microenvironment with vascularized stromal tissue. CAM assay is a well-established assay that has long been used as an *in vivo* environment to study tumor angiogenesis, invasion, and metastasis. Recent experimental findings have demonstrated that the PDX model utilizing CAM assay enables tumor progression and metastasis.

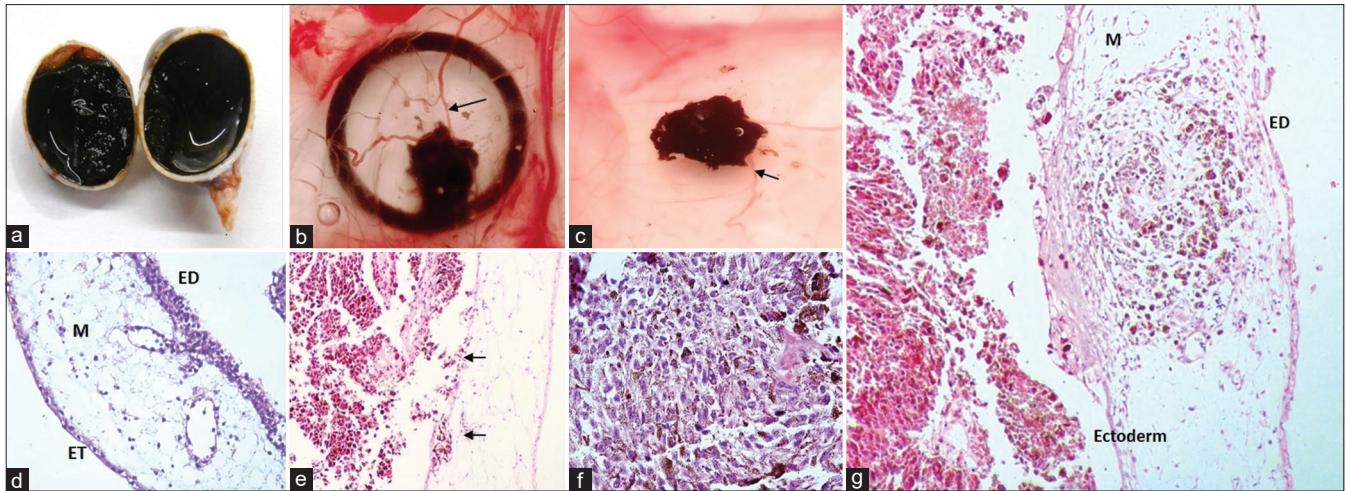


**Figure 2:** (a) Gross image of CM. (b) CM xenograft induced angiogenesis (arrow) on the area of implantation on the CAM. (c) CM xenograft on CAM (top view) with surrounding blood vessels (arrow). (d) Normal CAM revealing ET, M, and ED (H/E,  $\times 200$ ). (e) CM tumor attached on the ectoderm of CAM (arrow) (H/E,  $\times 200$ ). (f) Representative CM sample with spindle-shaped tumor cells arranged in fascicles with a moderate melanin pigment (H/E,  $\times 400$ ). (g) Histologic section revealing pigmented CM in the mesoderm of the chick CAM (H/E,  $\times 200$ ). CAM = chorioallantoic membrane, CM = choroidal melanoma, ED = endoderm, ET = ectoderm, H/E = hematoxylin and eosin, M = mesoderm

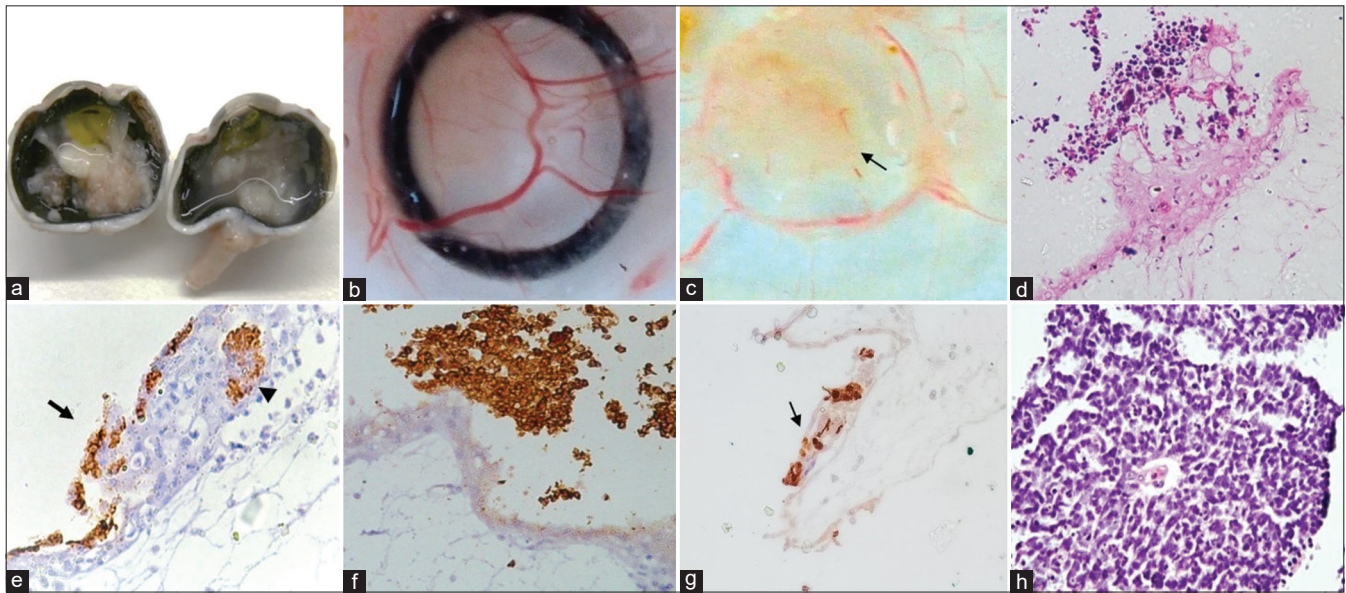


**Figure 3:** (a) Gross image of retinoblastoma. (b) Appearance of CAM along with retinoblastoma PDX showing high vascularity under the tumor implant site. (c) Implanted retinoblastoma PDX (arrow) on the CAM. (d) Retinoblastoma cells adhered to the CAM (H/E,  $\times 200$ ). (e) Synaptophysin-positive retinoblastoma cells attached to the ectoderm of CAM (arrow) and in CAM mesoderm (arrowhead) ( $\times 200$ ). (f) Synaptophysin positivity in retinoblastoma PDX on the surface of CAM ( $\times 200$ ). (g) Ki-67 immunostaining in retinoblastoma PDX on CAM epithelium ( $\times 200$ ). (h) Poorly differentiated retinoblastoma (H/E,  $\times 400$ ). CAM = chorioallantoic membrane, H/E = hematoxylin and eosin, PDX = patient-derived xenograft

The applications of CAM assay to investigate the invasive properties of aggressive ocular tumors are limited. So far, most published papers have relied on tumor cell lines instead of fresh PDXs. In the study presented here, we observed that both CM and RB fresh tumor tissues, when placed over CAM, resulted in high vascularization in the surrounding region, followed by the migration and invasion into the CAM mesoderm. The invasive properties of patient-derived cancer cells has been reported for many malignancies including Renal cell carcinoma (RCC), sarcoma, pancreatic adenocarcinoma, and ovarian carcinoma.<sup>[30-34]</sup> The use of CAM assay to demonstrate the

invasive properties of CM and RB PDX has not been reported to the best of our knowledge.

In this study, we have established successful growth of patient-derived CM and RB tissues and their invasion in CAM. Both the tumor tissue grafts showed a consistent adherence on the endodermal surface of CAM and cell division in all setups. The invasion was more prominent in CAM carrying CM PDXs. The tumor mass appeared to have invaded the CAM ectoderm and even formed tumor nodules in the CAM mesoderm. In the CAM carrying RB PDXs, close adherent connection between the

RB tumor and the CAM vasculature was grossly examined. The positivity of neural cell marker synaptophysin substantiated the presence of invasive RB cells. The invasion resulting in the destruction of the ectoderm followed by migration and invasion into the mesoderm has also been evidenced in various types of solid tumors such as ovarian carcinoma and nasopharyngeal carcinoma.<sup>[34,35]</sup> The successful relocation of tumor cells in these tumor types was used to examine the metastatic dissemination of cancer cells *in vivo*.

Recent work has ascertained the expansion of RB cells arising from the primary tumor on CAM in order to evaluate the effect of drugs. However, the invasive properties of RB cells were not demonstrated. Successful display of metastatic properties of UM has been illustrated using green fluorescent protein (GFP)-labeled OMM2 and 92.1 cell lines on CAM.<sup>[24]</sup> A recent publication has also utilized the CAM assay to explore the metastatic properties of RB cell lines (WERI-Rb1, Y-79, and RB 355).<sup>[36]</sup> The use of tumor fragments from patients offers numerous benefits over cell lines. PDX retains morphological similarity and conserves heterogeneity of tumor cell subpopulations. On the other hand, cell lines harbor negligible resemblance and, therefore, cause vast disparities between preclinical efficacy and clinical responses.<sup>[37]</sup> Studies investigating laryngeal squamous cell carcinoma have revealed that the CAM-invading cells preserved the original tumor characteristics and did not show any signs of necrosis till EDD 17.<sup>[28]</sup>

The histologic analysis of the CM-CAM graft uncovered that the tumor nodule within the mesoderm had retained phenotypic characteristics, implying that both the implanted tumor tissue and the invasive cells retained the properties of the original tumor. Similarly, the invasive RB cell in CAM also expressed synaptophysin, indicating the immunophenotypic character of the RB tumor. The aggressiveness of the RB tumor, on the other hand, is indicated by the strong Ki-67 immunopositivity.

The successful grafting and migration of CM and RB PDXs in the chick CAM assay make it a robust technique to monitor the invasion of aggressive ocular tumors. Comparison between CAM-invading tumor and original tumor xenograft and their properties can be made definitive in subsequent research using metrics like gene expression patterns, copy number alterations, and other investigative techniques. Hence, this study shows that the CAM assay can be utilized to analyze fresh CM and RB samples as a xenograft model.

## Conclusion

The current study allowed us to successfully envision the establishments of CM and RB PDXs on CAM for the period between EDD 10 and EDD 17, after which histopathologic and immunohistochemical analyses were performed. This analysis revealed high vascularization, adherence of tumor cells to CAM ectoderm, as well as invasion by tumor cells into the CAM mesoderm; however, the degree of invasion was more in case of CM when compared to RB. These outcomes feature the remarkable potential of CAM assay over conventional models: the chorioallantois is immunodeficient till EDD 13–14, allowing the growth of tumor xenografts without eliciting an immune response, the setup is time and cost effective, and poses almost no ethical objections. Furthermore, the resemblance

of CAM assay to the patient tumor microenvironment, with use of patient-derived tumors, makes it a potential model to develop personalized medicine for patients suffering from ocular cancer.

## Acknowledgements

The authors are grateful to Shivaji College, University of Delhi, for providing laboratory facilities and Dr. R. P. Centre, All India Institute of Medical Sciences, for providing tumor specimens and permission to use instruments for imaging and analytical testing. The authors also extend their sincere appreciation to the principal of Sri Venkateswara College and the principal and laboratory staff of Shivaji College.

## Financial support and sponsorship

Nil.

## Conflicts of interest

There are no conflicts of interest.

## References

1. Fiorentzis M, Viestenz A, Siebolts U, Seitz B, Coupland SE, Heinzelmann J. The potential use of electrochemotherapy in the treatment of uveal melanoma: *In vitro* results in 3D tumor cultures and *in vivo* results in a chick embryo model. *Cancers (Basel)* 2019;11:1344.
2. Shields CL, Furuta M, Thangappan A, Nagori S, Mashayekhi A, Lally DR, et al. Metastasis of uveal melanoma millimeter-by-millimeter in 8033 consecutive eyes. *Arch Ophthalmol* 2009;127:989–98.
3. van der Kooij MK, Speetjens FM, van der Burg SH, Kapiteijn E. Uveal versus cutaneous melanoma; same origin, very distinct tumor types. *Cancers (Basel)* 2019;11:E845.
4. Coupland SE, Lake SL, Zeschnigk M, Damato BE. Molecular pathology of uveal melanoma. *Eye (Lond)* 2013;27:230–42.
5. Kaliki S, Shields CL, Shields JA. Uveal melanoma: Estimating prognosis. *Indian J Ophthalmol* 2015;63:93–102.
6. Hamza HS, Elhousseiny AM. Choroidal melanoma resection. *Middle East Afr J Ophthalmol* 2018;25:65–70.
7. Brady LW, Hernandez JC. Brachytherapy of choroidal melanomas. *Strahlenther Onkol* 1992;168:61–5.
8. Retinoblastoma - The Lancet. Available from: [https://www.thelancet.com/article/S0140-6736\(11\)61137-9/fulltext](https://www.thelancet.com/article/S0140-6736(11)61137-9/fulltext). [Last accessed on 2022 Jun 08].
9. Dimaras H, Corson TW, Cobrinik D, White A, Zhao J, Munier FL, et al. Retinoblastoma. *Nat Rev Dis Primers* 2015;1:15021.
10. Cocarta AI, Hobzova R, Sirc J, Cerna T, Hrabeta J, Svojr K, et al. Hydrogel implants for transscleral drug delivery for retinoblastoma treatment. *Mater Sci Eng C Mater Biol Appl* 2019;103:109799.
11. Bremner R, Sage J. The origin of human retinoblastoma. *Nature* 2014;514:313.
12. Kletke SN, Feng ZX, Hazrati LN, Gallie BL, Soliman SE. Clinical predictors at diagnosis of low-risk histopathology in unilateral advanced retinoblastoma. *Ophthalmology* 2019;126:1306–14.
13. Ishaq H, Patel BC. Retinoblastoma. In: *StatPearls. Treasure Island (FL): StatPearls Publishing; 2022.*
14. Yang H, Cao J, Grossniklaus HE. Uveal melanoma metastasis models. *Ocul Oncol Pathol* 2015;1:151–60.
15. Richards JR, Yoo JH, Shin D, Odelberg SJ. Mouse models of uveal melanoma: Strengths, weaknesses, and future directions. *Pigment Cell Melanoma Res* 2020;33:264–78.
16. Tschulakow AV, Schraermeyer U, Rodemann HP, Julien-Schraermeyer S. Establishment of a novel retinoblastoma

- (Rb) nude mouse model by intravitreal injection of human Rb Y79 cells – Comparison of *in vivo* analysis versus histological follow up. *Biol Open* 2016;5:1625–30.
17. Liu M, Wang SM, Jiang ZX, Lauren H, Tao LM. Effects of miR-22 on viability, migration, invasion and apoptosis in retinoblastoma Y79 cells by targeting high-mobility group box 1. *Int J Ophthalmol* 2018;11:1600–7.
  18. Nair RM, Balla MMS, Khan I, Kalathur RKR, Kondaiah P, Vemuganti GK. *In vitro* characterization of CD133lo cancer stem cells in Retinoblastoma Y79 cell line. *BMC Cancer* 2017;17:779.
  19. Lei ZG, Ren XH, Wang SS, Liang XH, Tang YL. Immunocompromised and immunocompetent mouse models for head and neck squamous cell carcinoma. *Oncotargets Ther* 2016;9:545–55.
  20. Justus CR, Leffler N, Ruiz-Echevarria M, Yang LV. *In vitro* cell migration and invasion assays. *J Vis Exp* 2014;(88):51046.
  21. Staton CA, Reed MWR, Brown NJ. A critical analysis of current *in vitro* and *in vivo* angiogenesis assays. *Int J Exp Pathol* 2009;90:195–221.
  22. Metcalfe J, Stock MK. Oxygen exchange in the chorioallantoic membrane, avian homologue of the mammalian placenta. *Placenta* 1993;14:605–13.
  23. Lokman NA, Elder ASF, Ricciardelli C, Oehler MK. Chick chorioallantoic membrane (CAM) assay as an *in vivo* model to study the effect of newly identified molecules on ovarian cancer invasion and metastasis. *Int J Mol Sci* 2012;13:9959–70.
  24. Kalirai H, Shahidipour H, Coupland SE, Luyten G. Use of the chick embryo model in uveal melanoma. *Ocul Oncol Pathol* 2015;1:133–40.
  25. Busch M, Philippeit C, Weise A, Dünker N. Re-characterization of established human retinoblastoma cell lines. *Histochem Cell Biol* 2015;143:325–38.
  26. Miserocchi G, Mercatali L, Liverani C, De Vita A, Spadazzi C, Pieri F, *et al.* Management and potentialities of primary cancer cultures in preclinical and translational studies. *J Transl Med* 2017;15:229.
  27. Li M, Pathak RR, Lopez-Rivera E, Friedman SL, Aguirre-Ghiso JA, Sikora AG. the *in ovo* chick chorioallantoic membrane (CAM) assay as an efficient xenograft model of hepatocellular carcinoma. *J Vis Exp* 2015;(104):52411.
  28. Uloza V, Kuzminienė A, Šalomskaitė-Davalgienė S, Palubinskienė J, Balnytė I, Ulozienė I, *et al.* Effect of laryngeal squamous cell carcinoma tissue implantation on the chick embryo chorioallantoic membrane: Morphometric measurements and vascularity. *BioMed Res Int* 2015;2015:629754.
  29. Kauffmann P, Troeltzsch M, Brockmeyer P, Bohnenberger H, Heidekrüger PI, Manzke M, *et al.* First experience of chick chorioallantoic membrane (CAM) assay in the clinical work flow with oral squamous cell carcinoma patients. *Clin Hemorheol Microcirc* 2018;70:487–94.
  30. Fergelot P, Bernhard JC, Soulet F, Kilarski WW, Léon C, Courtois N, *et al.* The experimental renal cell carcinoma model in the chick embryo. *Angiogenesis* 2013;16:181–94.
  31. Sys GML, Lapeire L, Stevens N, Favoreel H, Forsyth R, Bracke M, *et al.* The *in ovo* CAM-assay as a xenograft model for sarcoma. *J Vis Exp* 2013;(77):e50522.
  32. Rovithi M, Avan A, Funel N, León L, Gómez Mellado V, Wurdinger T, *et al.* Development of bioluminescent chick chorioallantoic membrane (CAM) models for primary pancreatic cancer cells: A platform for drug testing. *Sci Rep* 2017;7:44686.
  33. Hu J, Ishihara M, Chin AI, Wu L. Establishment of xenografts of urological cancers on chicken chorioallantoic membrane (CAM) to study metastasis. *Precis Clin Med* 2019;2:140–51.
  34. Ismail MS, Torsten U, Dressler C, Diederichs JE, Hüske S, Weitzel H, *et al.* Photodynamic therapy of malignant ovarian tumours cultivated on CAM. *Lasers Med Sci* 1999;14:91–6.
  35. Xiao X, Zhou X, Ming H, Zhang J, Huang G, Zhang Z, *et al.* Chick chorioallantoic membrane assay: A 3D animal model for study of human nasopharyngeal carcinoma. *PLoS One* 2015;10:e0130935.
  36. Busch M, Papior D, Stephan H, Dünker N. Characterization of etoposide- and cisplatin-chemoresistant retinoblastoma cell lines. *Oncol Rep* 2018;39:160–72.
  37. Dagogo-Jack I, Shaw AT. Tumour heterogeneity and resistance to cancer therapies. *Nat Rev Clin Oncol* 2018;15:81–94.